

Hydra: Multi-head Low-rank Adaptation for Parameter Efficient Fine-tuning

Sanghyeon Kim^{1*} Hyunmo Yang^{2*} Younghyun Kim^{2*} Youngjoon Hong^{3†}
 Eunbyung Park^{1,2†}

¹Department of Electrical and Computer Engineering, Sungkyunkwan University

²Department of Artificial Intelligence, Sungkyunkwan University

³Department of Mathematical Sciences, KAIST

Abstract

The recent surge in large-scale foundation models has spurred the development of efficient methods for adapting these models to various downstream tasks. Low-rank adaptation methods, such as LoRA, have gained significant attention due to their outstanding parameter efficiency and no additional inference latency. This paper investigates a more general form of adapter module based on the analysis that parallel and sequential adaptation branches learn novel and general features during fine-tuning, respectively. The proposed method, named Hydra, due to its multi-head computational branches, combines parallel and sequential branch to integrate capabilities, which is more expressive than existing single branch methods and enables the exploration of a broader range of optimal points in the fine-tuning process. In addition, the proposed adaptation method explicitly leverages the pre-trained weights by performing a linear combination of the pre-trained features. It allows the learned features to have better generalization performance across diverse downstream tasks. Furthermore, we perform a comprehensive analysis of the characteristics of each adaptation branch with empirical evidence. Through an extensive range of experiments, encompassing comparisons and ablation studies, we substantiate the efficiency and demonstrate the superior performance of Hydra. This comprehensive evaluation underscores the potential impact and effectiveness of Hydra in a variety of applications. Our code is available on <https://github.com/extremebird/Hydra>

1. Introduction

The large-scale foundation models have been remarkably successful across a broad range of domains and tasks [5, 12, 15, 40, 61]. Training these large-scale models from scratch is a formidable task, primarily limited to

*Equal contributions

†Corresponding authors

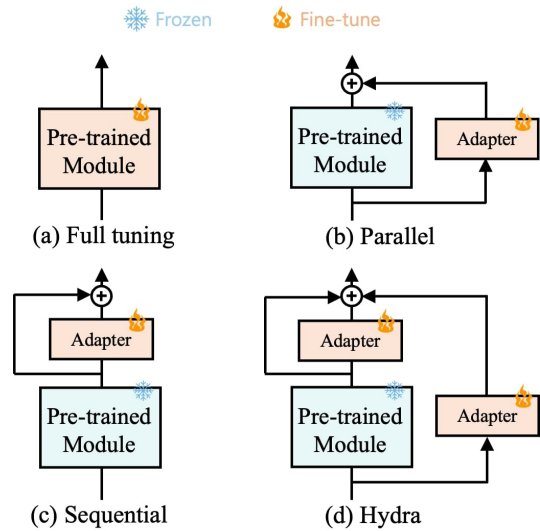


Figure 1. Graphical illustration of the model adaptation approaches. (a) fully updates *all* model parameters. (b) and (c) utilize adapter module either in a parallel or a sequential manner. (d) Hydra leverages both parallel and sequential adapter.

a selected few organizations. The main obstacles hindering broader accessibility are the substantial model sizes, exorbitant computational requirements, and the unavailability of extensive datasets. In particular, a large model size imposes a significant computational burden even during fine-tuning for downstream tasks. Efficiently adapting these large-scale models to downstream tasks has emerged as the prevailing practice in numerous applications.

Parameter Efficient Fine-tuning (PEFT) methods [7, 32–34, 47, 48, 80] efficiently fine-tune a pre-trained network. Although these methods optimize a significantly smaller number of parameters than the total parameters, they have outperformed the full tuning in various downstream tasks. Among PEFT methods, adapter-based methods [7, 32, 33, 48] have demonstrated superior performance and been widely used. They attach lightweight modules,

called adapter, to a pre-trained model and optimize only the adapter modules during fine-tuning. Recently, motivated by empirical evidence of low intrinsic dimension in model adaptation, LoRA [33] leverages linear adapter modules to eliminate the additional inference latency existed in previous adapter-based methods [7, 32]. Furthermore, various matrix factorization techniques have been applied to adapter modules to enhance efficiency [29, 82].

While adapter-based methods have become more efficient and advanced, they have been limited to either a parallel or a sequential approach. The parallel (Fig. 1-(b)) and sequential (Fig. 1-(c)) approaches are represented as $f(x) + g(x)$ and $f(x) + g(f(x))$, respectively, where f is a pre-trained module and g is an adapter module. While these two are expressed in a similar fashion, the adapter module of each approach is optimized with different features, x and $f(x)$, as inputs. In other words, task-specific features can be acquired based on how the adapter module is attached during fine-tuning. However, existing adapter-based methods have not extensively explored this aspect.

This paper investigates the characteristics of each attachment approach. The parallel branch is optimized over the same input x as the pre-trained layer, leading to the learning of task-specific features that have not been pre-trained. This aligns well with the empirical observations, as previous study [33] found that low-rank adaptation often amplifies the important features relevant to specific downstream tasks. On the other hand, the sequential branch learns to combine general features from the pre-trained large-scale model due to its explicit formulation $g(f(x))$.

Based on these characteristics, we propose a more general form of adapter module, called *Hydra*¹, combining parallel and sequential adapter modules. The proposed form is $f(x) + g_p(x) + g_s(f(x))$, where g_p and g_s are parallel and sequential adapter, respectively. This formulation is inherently more expressive than single branch approaches, as it can be reduced to one of them when $g_p(\cdot) = 0$ or $g_s(\cdot) = 0$. Our hypothesis is that the introduction of a more general and expressive form enables the exploration of a broader range of local optima. Consequently, this increased flexibility may lead to superior generalization performance for the new tasks.

In addition, we use the linear adapter module of LoRA to construct the proposed method while preserving its advantageous properties. Therefore, the two additional computational branches of our method can be merged after training, hence no additional latency during inference. Moreover, thanks to the simple and versatile linear adapter structure, the proposed module can not only be easily implemented but also be plugged into any linear layers for parameter efficient fine-tuning purposes.

¹Named after the multi-headed Greek mythological beast, rhyme with the original LoRA

In this paper, we deeply delve into the role of both parallel and sequential branches. We observe that each branch learns distinct features during fine-tuning. To elaborate, the parallel branch tends to learn new features by exploring features that were absent during the pre-training phase, and the sequential branch relatively general features by exploiting pre-trained features. The proposed method, *Hydra*, has undergone extensive testing on popular transformer architectures, and we have conducted fine-tuning experiments on diverse datasets spanning vision and natural language tasks. As a result, leveraging both parallel and sequential branches further increases the fine-tuning ability of the model, surpassing other prevalent fine-tuning methods.

2. Related works

2.1. Transformer

Transformer is a neural network architecture that uses multi-head self attention layers and was initially proposed for machine translation [71]. Many large-scale pre-trained transformers [5, 15, 45, 50, 60, 61] have exhibited outstanding performance on numerous natural language processing (NLP) tasks, indicating their scalability. These successes of transformers in NLP fields inspired [18] to introduce the Vision Transformer (ViT), a purely transformer-based backbone architecture for computer vision (CV) tasks that demonstrated promising results. Subsequently, many transformer-based vision models [12, 17, 51, 69] have been suggested and shown significant improvement on vision tasks, including image classification [13, 42], dense prediction [49, 84], and image generation [31, 38]. Moreover, multi-modal training [59] and self-supervised learning [28] also accelerate the broad use of ViT. In this paper, we apply our method to transformer architectures widely used in both language and vision tasks.

2.2. Adapter-based methods

Adapter-based method is one of the parameter-efficient adaptation methods that involve training only lightweight adapter modules without updating the original parameters of a pre-trained model. [63] is a pioneer work that applied adapter modules for multiple vision domain adaptation. Adapter [32] introduced a low-rank residual adapter module that consists of down and up projection with intermediate non-linear function.

Subsequent studies [1, 58, 64] demonstrated promising and efficient fine-tuning performance in various NLP tasks. Moreover, Compacter [37] leveraged the Kronecker product decomposition and parameter sharing to the projection matrices of adapter modules for more efficient adaptation. VL-adapter [68] successfully applied various adapters to multi-modal (vision and language) tasks, demonstrating their versatility and effectiveness. Adaptorformer [7] introduced a

parallel adapter to feed-forward networks of ViT for visual recognition tasks. While these adapter tuning methods demonstrated promising results, the additional adapter branches, which have intermediate non-linear functions, slow down the inference speed.

LoRA [33] proposed a low-rank adaptation module composed solely of linear layers. This design allows the parameters of introduced branches to be merged in an additive manner with the pre-trained parameters at the inference stage, ensuring no latency. Compared to existing adapter tuning, it has shown competitive or even better adaptation ability in NLP fields. AdaLoRA [82] further improved LoRA with singular value decomposition (SVD) for adaptive budget allocation. KAdaptation [29] leveraged a low-rank weight update manner similar to LoRA, in which the update weights are obtained by Kronecker product of shared matrix and low-rank matrix, for fine-tuning vision models. Also, FacT [35] proposed tensorization-decomposition framework, which tensorize whole ViT into a single 3D tensor, then apply Factor-Tuning with various tensor decomposition methods, such as Tensor-Train(TT) or Tucker(TK). SSF [48] suggested the introduction of scaling and shifting factors to perform linear transformation on features after pre-trained modules of ViT, in order to match the target distribution. Recently, RepAdapter [52] proposed a sequential structural reparameterization scheme for low-rank adaptation modules. These studies have exhibited competitive performance and efficiency, not sagging the inference speed. Building upop these single branch approaches, we leverage parallel and sequential branches together to demonstrate superior performance.

2.3. Other PEFT approaches

Besides the success of adapter-based methods, the approaches without adapter have been explored. BitFit [80] only trained bias-terms during fine-tuning. Diff-pruning [26] introduced a task-specific diff vector, which is adaptively pruned during training. Token-based tuning approaches [34, 44, 47, 65] also widely used PEFT methods. They involves attaching supplementary tokens, also known as prompt, to the input or intermediate sequence and fine-tune them to guide the model’s attention towards the relevant information for the new task. VPT [34] demonstrated promising performance in vision domain by applying the prompt tuning approach that succeeded in natural language tasks. While token-based tuning has demonstrated promising tuning ability, the addition of new tokens causes a few drawbacks. It reduces the available input sequence length, potentially limiting the amount of context that the model can process effectively. Moreover, it increases computational complexity. Moreover, applying these approaches to models that utilize local self-attention can pose additional challenges.

3. Methods

3.1. Preliminary

LoRA [33] applies a linear adapter module on linear (dense) layers of a pre-trained model for efficient model adaptation. It assumes that the intrinsic rank of adaptation matrix $A \in \mathbb{R}^{d \times k}$ is low, allowing a low-rank decomposition on A ($\text{rank}(A) \ll \min(d, k)$). That is, the adaptation matrix A is decomposed as $A = A_{\text{up}}A_{\text{down}}$, where $A_{\text{up}} \in \mathbb{R}^{d \times r}$ and $A_{\text{down}} \in \mathbb{R}^{r \times k}$ are an up-projection and down-projection adaptation matrix, respectively. Thus, the linear adapter module is formulated as $g(x; A_{\text{up}}, A_{\text{down}}) = A_{\text{up}}A_{\text{down}}x$. For brevity, henceforth, we use $g(x; A)$ to denote $g(x; A_{\text{up}}, A_{\text{down}})$

For a given input feature $x \in \mathbb{R}^k$, the forward pass of LoRA is implemented as below:

$$h = f(x; W_0, b_0) + g(x; A) \quad (1)$$

$$= W_0x + b_0 + A_{\text{up}}A_{\text{down}}x, \quad (2)$$

where $h \in \mathbb{R}^d$ is an output vector, $W_0 \in \mathbb{R}^{d \times k}$ is a pre-trained weight matrix, and $b_0 \in \mathbb{R}^d$ is a bias. To efficiently optimize the linear layer during fine-tuning, only the adaptation matrices A_{up} and A_{down} are trained, and the pre-trained matrix W_0 and bias b_0 are frozen. While using the extra parallel branch $g(x; A)$ is efficient for fine-tuning, it leads latency in inference. Thanks to the linearity, the forward pass in Eq. (2) can be re-implemented as follow:

$$h = (W_0 + A)x + b_0 \quad (3)$$

$$= f(x; W_0 + A, b_0), \quad (4)$$

In other words, during inference, the adapter module can be merged into the pre-trained linear layer, ensuring no additional computational cost.

In Eq. (1), it is evident that LoRA is one of the parallel approaches. The linear adapter module of LoRA can be optimized without direct dependence on the pre-trained matrix W_0 . Therefore, it would facilitates the ease of learning new features that diverge from the pre-trained features. However, there is a possibility of losing the generalization ability of pre-trained weight matrix.

3.2. SeqLoRA

In order to compare parallel and sequential approaches, we introduce SeqLoRA, a sequential form of LoRA, leveraging the idea of a low-rank adaptation on an output vector of the pre-trained linear layer. This results in the following forward pass:

$$h = f(x; W_0, b_0) + g(f(x; W_0, b_0); B) \quad (5)$$

$$= W_0x + b_0 + B_{\text{up}}B_{\text{down}}W_0x + B_{\text{up}}B_{\text{down}}b_0, \quad (6)$$

where $B \in \mathbb{R}^{d \times d}$ is an adaptation matrix, $B_{\text{up}} \in \mathbb{R}^{d \times r}$ is an up-projection adaptation matrix, and $B_{\text{down}} \in \mathbb{R}^{r \times d}$ is a

down-projection adaptation matrix. Similar to LoRA, only the adapter module is optimized and the forward pass for inference can be represented as a single linear layer:

$$h = (W_0 + BW_0)x + b_0 + Bb_0 \quad (7)$$

$$= f(x; W_0 + BW_0, b_0 + Bb_0), \quad (8)$$

We posit that LoRA and SeqLoRA are complementary to each other. SeqLoRA can learn new features for the downstream tasks by linearly combining features from the pre-trained layer. While SeqLoRA has the capacity to learn highly useful features based on the capabilities of the large-scale pre-trained models, it may encounter limitations in learning novel concepts or features that were absent during the pre-training phase.

SeqLoRA shares similarities with the recently proposed RepAdapter [52] in terms of its sequential linear adapter module. However, we introduce it to compare with its parallel counterpart and utilize a component of following our proposed method, *Hydra*.

3.3. Hydra

To harness the strengths of both LoRA and SeqLoRA, we introduce *Hydra*, a more general form of linear adaptation module that integrates the capabilities of both methods. *Hydra* allows for the combination and utilization of the advantageous aspects of LoRA and SeqLoRA, providing a comprehensive and flexible framework for efficient and effective model adaptation. More precisely, it can not only capture novel features easily but also get a broader sight based on general pre-trained features. For *Hydra*, we combine parallel and sequential adaptation branches, which allows us the following forward pass:

$$h = f(x; W_0, b_0) + g(x; A) + g(f(x; W_0, b_0); B) \quad (9)$$

$$= W_0x + b_0 + A_{\text{up}}A_{\text{down}}x + B_{\text{up}}B_{\text{down}}W_0x + B_{\text{up}}B_{\text{down}}b_0, \quad (10)$$

where $A \in \mathbb{R}^{d \times k}$, $A_{\text{up}} \in \mathbb{R}^{d \times r_a}$, $A_{\text{down}} \in \mathbb{R}^{r_a \times k}$ is an adaptation matrix for parallel branch and its low-rank decomposition with rank r_a , $B \in \mathbb{R}^{d \times d}$, $B_{\text{up}} \in \mathbb{R}^{d \times r_b}$, $B_{\text{down}} \in \mathbb{R}^{r_b \times d}$ is an adaptation matrix for sequential branch and its low-rank decomposition with rank r_b . For simplicity, we set rank as $r_a = r_b$ throughout the paper. Following LoRA, we use a random Gaussian initialization for down-projection matrices, A_{down} and B_{down} , and zero initialization for up-projection matrices, A_{up} and B_{up} . Consequently, at the start of the training, both A and B are initialized to zero. For model adaptation, A_{up} , A_{down} , B_{up} , and B_{down} are trained based on the gradient descent, while W_0 and b_0 are not updated.

As depicted in Fig. 1-(d), the implementation for training consists of three branches: pre-trained, parallel, and sequential. After the training, parallel and sequential branches

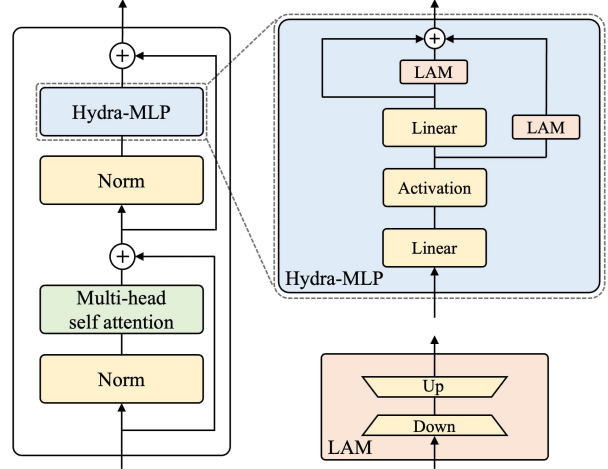


Figure 2. *Hydra*-MLP in a transformer architecture in the training phase. Linear Adapter Module (LAM) implements down projection and up projection on its input in order.

can be merged into the pre-trained branch as follows:

$$h = (W_0 + A + BW_0)x + b_0 + Bb_0 \quad (11)$$

$$= f(x; W_0 + A + BW_0, b_0 + Bb_0), \quad (12)$$

Therefore, our method does not increase computational complexity during inference.

In addition, it is apparent that LoRA and SeqLoRA can be identified as specific instances of *Hydra* when $B = 0$ and $A = 0$, respectively. This observation establishes that our method encompasses a more generalized framework for task-specific adaptations. As a result, our approach provides an enhanced modeling capacity to comprehensively capture various adaptation scenarios during fine-tuning.

3.4. Architecture design

While our approach is designed to be compatible with any linear layers, in this work, we focus on its application to the MLP blocks within transformer architectures, which have been widely used in recent large-scale models. As illustrated in Fig. 2, a typical transformer block consists of a multi-head self attention (MSA) block and an MLP block, interleaved by non-linear activations and layer normalization. We replace the proposed adaptation module with the last layer of the MLP block. Since non-linear activations are not employed in the final linear layer of the MLP, we can avoid the potential ‘additional latency’ that could arise during the inference. We refer to the MLP block, to which our method is applied, as *Hydra*-MLP.

In addition, this design choice is also motivated by recent studies, revealing that self-attention blocks in the transformers tend to diminish high-frequency information, whereas MLP blocks amplify it [56, 75]. As *Hydra*-MLP contains

Method	#Params (M)	Avg Acc. (↑)	PE (↑)	Caltech101	CIFAR10	CIFAR100	Country211	DTD	EuroSAT	FER2013	FGVCAircraft	Food101	GTSRB	HatefulMemes	KITTI-Dist	MNIST	Flowers102	OxfordPets	PatchCamelyon	SST2	Resisc45	StanfordCars	VOC2007
Full tuning	87.9	65.49	0.498	87.64	91.11	71.52	15.75	54.36	85.24	52.72	26.22	83.28	74.05	55.64	39.15	65.55	80.55	87.31	64.92	59.09	75.61	57.21	82.95
Linear-probing	0.03	66.32	0.663	90.96	90.35	67.31	17.36	62.04	72.95	51.91	29.52	83.82	56.47	55.83	40.37	77.50	92.29	88.03	59.00	59.36	78.10	68.30	84.99
Adapter [32]	1.24	65.08	0.647	90.18	90.14	73.57	16.83	57.13	67.97	41.76	30.52	83.58	58.50	48.91	37.18	80.34	90.78	86.52	59.92	58.70	79.22	67.68	82.22
LoRA [33]	0.18	61.48	0.614	87.64	90.52	69.69	17.12	50.16	74.03	51.04	20.01	83.76	42.96	55.88	48.05	61.36	74.28	85.49	63.20	57.04	62.09	54.89	80.33
Compacter [37]	0.08	62.79	0.628	89.02	79.96	44.33	28.22	52.93	50.48	35.46	41.13	78.28	66.90	47.60	57.72	85.82	88.29	79.23	61.83	64.22	63.76	64.79	75.84
Kadapation [29]	0.08	68.92	0.689	88.96	90.03	73.92	17.53	63.97	76.25	47.45	30.04	84.38	80.71	55.86	42.29	85.20	93.19	89.05	63.39	59.18	79.96	70.21	84.49
Hydra	0.20	70.95	0.709	91.23	90.89	74.20	17.75	64.47	87.00	51.10	33.05	84.27	87.11	55.91	42.05	90.76	93.18	89.38	70.83	59.58	82.41	71.19	82.66

Table 1. ELEVATER experiment results. We use CLIP pre-trained ViT-Base-224/32 as a backbone model.

SeqLoRA that is designed to exploit the pre-trained features through the linear combination, our approach effectively encourages the model to promote useful high-frequency features for specific downstream tasks. Unless specified, in this paper, *Hydra* indicates *Hydra*-MLP.

4. Experimental results

We substantiate the versatility of our method *Hydra* through an extensive range of experiments including both vision and natural language tasks. Next, we analyze the characteristics based on the utilization approach of adapter branch and discuss the computational efficiency of the proposed method. Finally, we verify the effectiveness of our architecture design by conducting ablation studies.

4.1. Few-shot experiments

First, since various fine-tuning applications opt to fall down to the condition of limited data accessibility, we validated our proposed *Hydra* in a few-shot learning scenario using 20 image classification datasets from the ELEVATER benchmark [46]. Each dataset comprises a distinct number of labels along their corresponding images. Following the previous work [29], we used the CLIP pre-trained ViT-Base-224/32 as a backbone model. And, we set the bottleneck rank of *Hydra* as $r_a = r_b = 2$. Detailed experimental settings and statistics of each dataset are reported in Appendices B and C, respectively.

As shown in Tab. 1, *Hydra* achieved the highest accuracy score on 11 out of 20 datasets and surpassed the other PEFT methods with regard to the average accuracy. Furthermore, we report the PE score [46] to compare accuracy-efficiency trade-off. The PE score is defined as follow:

$$PE = \text{accuracy} \cdot \exp(-\log_{10}(p/M_0 + 1)), \quad (13)$$

where p is the number of trainable parameters, and M_0 is a magnitude of pre-trained model’s parameters. We set $M_0 = 10^8$. We observed that our method also attained the highest

PE score in Tab. 1. As a result, the proposed method is not only effective but also efficient for few-shot learning.

4.2. VTAB-1k experiments

Next, we conducted the experiment on the VTAB-1k benchmark [81] to compare *Hydra* with the state-of-the-art PEFT methods. The VTAB-1k benchmark consists 19 vision datasets and each dataset are categorized into three groups with different concepts, i.e., the *Natural*, *Specialized* and *Structured*. We used ViT-Base-224/16 model pre-trained on ImageNet-21k in a supervised manner. Following prior works [52], we applied our *Hydra* module on every layer of both projection layer in attention block and final linear layer of MLP block with low-rank dimension $r_a = r_b = 2$ for this experiment. More details of the experiments are in Appendices B and C.

We noted that *Hydra* excels recent PEFT methods in Tab. 2. Compared to existing non-linear adapter methods [7, 32], our method has demonstrated enhanced performance, avoiding any additional inference latency through the combination of linear operations. Therefore this signifies linear adapter modules can also function well in a multi-branch approach.

Furthermore, it is noteworthy the proposed method, which combines parallel and sequential adaptation branches, outperforms previous single branch (either parallel or sequential) approaches [33, 35, 48, 52]. To effectively learn task-specific feature during fine-tuning, in other words, both a parallel branch that learns novel concepts and a sequential branch that transforms pre-trained features need to be used in conjunction. As a result, introducing a more comprehensive and expressive structure is helpful for proficient task adaptation.

4.3. Natural language understanding experiments

In the field of NLP, transformers have achieved great success, leading numerous large-scale pre-trained transformer

Method	#Params (M)	Avg. Acc.	Natural							Specialized				Structured							
			CIFAR100	Caltech101	DTD	Flowers102	OxfordPets	SVHN	Sun397	PatchCamelyon	EuroSAT	Resisc45	Retinopathy	Clevr-Count	Clevr-Dist	DMLab	KITTI-Dist	dSPR-Loc	dSPR-Ori	sNORB-Azim	sNORB-Ele
Full tuning	85.8	68.9	68.9	87.7	64.3	97.2	86.9	87.4	38.8	79.7	95.7	84.2	73.9	56.3	58.6	41.7	65.5	57.5	46.7	25.7	29.1
Linear-probing	0.04	57.6	64.4	85.0	63.2	97.0	86.3	36.6	51.0	78.5	87.5	68.5	74.0	34.3	30.6	33.2	55.4	12.5	20.0	9.6	19.2
Adapter [32]	0.16	73.9	69.2	90.1	68.0	98.8	89.9	82.8	54.3	84.0	94.9	81.9	75.5	80.9	65.3	48.6	78.3	74.8	48.5	29.9	41.6
AdaptFormer [7]	0.16	74.7	70.8	91.2	70.5	99.1	90.9	86.6	54.8	83.0	95.8	84.4	76.3	81.9	64.3	49.3	80.3	76.3	45.7	31.7	41.1
LoRA [33]	0.29	74.5	67.1	91.4	69.4	98.8	90.4	85.3	54.0	84.9	95.3	84.4	73.6	82.9	69.2	49.8	78.5	75.7	47.1	31.0	44.0
VPT [34]	0.53	72.0	78.8	90.8	65.8	98.0	88.3	78.1	49.6	81.8	96.1	83.4	68.4	68.5	60.0	46.5	72.8	73.6	47.9	32.9	37.8
NOAH [83]	0.36	75.5	69.6	92.7	70.2	99.1	90.4	86.1	53.7	84.4	95.4	83.9	75.8	82.8	68.9	49.9	81.7	81.8	48.3	32.8	44.2
SSF [48]	0.22	75.7	69.0	92.6	75.1	99.4	91.8	90.2	52.9	87.4	95.9	87.4	75.5	75.9	62.3	53.3	80.6	77.3	54.9	29.5	37.9
FacT [35]	0.07	75.6	70.6	90.6	70.8	99.1	90.7	88.6	54.1	84.8	96.2	84.5	75.7	82.6	68.2	49.8	80.7	80.8	47.4	33.2	43.0
RepAdapter [52]	0.22	76.1	72.4	91.6	71.0	99.2	91.4	90.7	55.1	85.3	95.9	84.6	75.9	82.3	68.0	50.4	79.9	80.4	49.2	38.6	41.0
Hydra	0.28	76.5	72.7	91.3	72.0	99.2	91.4	90.7	55.5	85.8	96.0	86.1	75.9	83.2	68.2	50.9	82.3	80.3	50.8	34.5	43.1

Table 2. VTAB-1k experiment results. All methods are conducted by ViT-Base-224/16 pre-trained on ImageNet-21k.

Method	#Params (M)		MNLI	SST-2	MRPC	CoLA	QNLI	QQP	RTE	STS-B
	Avg.									
Full tuning	125	86.4	87.6	94.8	90.2	63.6	92.8	91.9	78.7	91.2
BitFit [80]	0.1	85.2	84.7	93.7	92.7	62.0	91.8	84.0	81.5	90.8
AdapterDrop [64]	0.3	84.4	87.1	94.2	88.5	60.8	93.1	90.2	71.5	89.7
AdapterDrop [64]	0.9	85.4	87.3	94.7	88.4	62.6	93.0	90.6	75.9	90.3
LoRA [33]	0.3	87.2	87.5	95.1	89.7	63.4	93.3	90.8	86.6	91.5
Hydra	0.3	87.9	87.5	95.0	92.2	65.4	92.8	90.8	87.4	91.7

Table 3. Natural language understanding results. We report the Matthew’s correlation for CoLA, Pearson correlation for STS-B, and accuracy for the others.

models. Hence, many PEFT methods were initially proposed for NLP tasks. Therefore, in this section, we validated that our method can effectively fine-tune a pre-trained NLP model as well. We performed natural language understanding experiments on GLUE benchmark [73]. Following [33], we used the pre-trained RoBERTa (base) [50], which originally has 125M trainable parameters from the HuggingFace Transformers library [78]. More experimental details are in Appendices B and C.

As shown in Tab. 3, *Hydra* has demonstrated superior adaptation capability compared to full tuning while requiring significantly fewer trainable parameters. Similarly, akin to results from vision task experiments, the pro-

posed method outperforms existing PEFT approaches. Notably, despite both LoRA and *Hydra* applying the same linear adapter module, *Hydra* achieves a substantial lead over LoRA, showing a significant performance advantage (+0.7 on average). This underscores the potential of the proposed method in NLP tasks as well. In essence, our multi-branch adapter module exhibits strong performance across domains, making it versatile and applicable in various fine-tuning scenarios.

4.4. Analysis

Adapter-based methods can be categorized into parallel and sequential approaches based on the attachment manner. While the formulations (Eqs. (1) and (5)) are similar, they are trained in distinct way because of different input features. The parallel branch learns new features by exploring features that were absent during the pre-training phase. On the other hand, the sequential branch learns relatively general features by exploiting pre-trained features. In this section, we delve into the attributes of the parallel and sequential branches with experimental evidence. Following that, we also analyze *Hydra* from the perspective of efficiency, an important element of the PEFT methods.

Subspace similarity of weight matrix We analyze each branch in terms of the weight matrix. To do so, we measured the similarity between pre-trained weight matrix W_0 and the weight matrices of each branch. In Eq. (11), the weight matrices of the parallel and sequential branches are represented as A and BW_0 , respectively, for input x . Fol-

lowing [33], we leveraged subspace similarity defined as below:

$$\phi(M, N, i, j) = \frac{\|U_M^i{}^T U_N^j\|_F^2}{\min\{i, j\}}, \quad (14)$$

where matrices $U_M^i \in \mathbb{R}^{d \times i}$ and $U_N^j \in \mathbb{R}^{d \times j}$ are formed by extracting from first to i -th and j -th columns of the left singular matrix of matrices M and N , respectively. We evaluated the similarity between the top 10% singular directions in the pre-trained matrix W_0 and the top 2 singular directions in the adaptation weight matrix A or BW_0 .

In Fig. 3, we observed higher overall similarity values between BW_0 and W_0 compared to A and W_0 due to explicitly leveraging W_0 . This indicates the sequential branch tends to learn general features that are relatively similar to pre-trained features. Furthermore, the majority of similarity values do not exceed 0.25 for both A and BW_0 . It implies the *Hydra* module enhances task-specific features instead of the previously amplified features by W_0 . Thus, our multi-branch module effectively fulfills the role of the adapter module, which needs to learn task-specific features.

Visualization of the feature space We conducted t-SNE [70] visualization on the embedding features of the [CLS] token in the last transformer block after fine-tuning. In this visualization, we visualized the embedding feature, distinguishing it into pre-trained branch output $f(x; W_0, b_0)$, parallel branch output $g(x; A)$, and sequential branch output $g(f(x; W_0, b_0); B)$. Based on this, we interpreted what features each branch is trained to represent.

As illustrated in Fig. 4, we can observe a notable difference in the distribution of output features between the parallel branch and the sequential branch. This clearly demonstrates that each branch hold distinct characteristics. In particular, the distribution of output features in the sequential branch primarily within the feature space of the pre-trained branch. It indicates that the sequential branch learns features that are similar to well-generalized pre-trained ones. On the other hand, the parallel branch learns the unique features that were not acquired during pre-training.

Method	#Params (M)	Training Time (sec/epoch)
Full tuning	85.8	148.95
LoRA	0.22	115.44
SeqLoRA	0.21	112.19
Hydra	0.21	119.37

Table 4. Training time comparison of full tuning, single branch approaches, and *Hydra* with CIFAR10 on a single RTX3090 GPU. The results are tested with a batch size of 128 and input resolution of 224×224 . Reported training time(sec/epoch) is the average across 10 epochs.

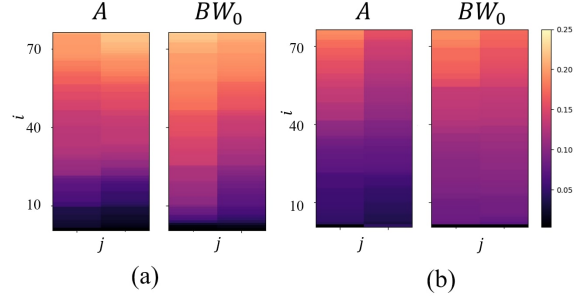


Figure 3. Normalized subspace similarity. $\phi(W_0, A, i, j)$ and $\phi(W_0, BW_0, i, j)$ of each transformer block trained on CIFAR100 in VTAB-1k benchmark. (a) and (b) correspond to the 6th and 9th blocks of ViT-Base-224/16, respectively.

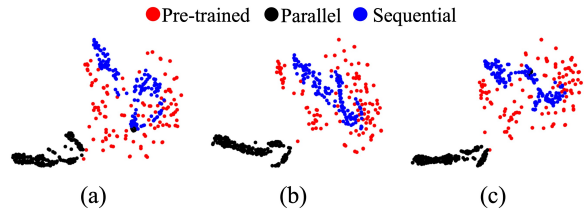


Figure 4. t-SNE visualizations of [CLS] token embedding. We used ViT-Base-224/32 trained on CIFAR100 in VTAB-1k benchmark. (a), (b), and (c) are the results of different random seeds, respectively. For each result, we used 128 images as input.

Computational efficiency Here, we address the parameter-efficiency of our *Hydra* with computational complexity. For simplicity, we assume the input and output of linear adapter module have the same dimension d . Then, the linear adapter module has a computational complexity of $O(2rd)$. This is because it is defined as $g(x; A) = A_{up}A_{down}x$, where $A_{up} \in \mathbb{R}^{d \times r}$, and $A_{down} \in \mathbb{R}^{r \times d}$. Therefore, the computational complexity of the single branch methods, LoRA and SeqLoRA, is $O(2rd)$. For $r_a = r_b = r$, *Hydra* fundamentally has two branches, leading to an increase in computational complexity. However, in all our experiments, we set $r_a = r_b = \frac{r}{2}$, resulting in both time and memory complexity of $O(2rd)$. It implies that the computational complexity of LoRA, SeqLoRA, and *Hydra* are theoretically identical.

However, when applied to the real applications, multi-branch design of *Hydra* is likely to lead bottlenecks on GPU. To figure out the bottlenecks, we compared the training time of each method on CIFAR10 dataset. For a fair comparison, we applied all methods, including *Hydra*, to MLP blocks. We used ViT-Base-224/32 model with batch size of 128. The results are shown in Tab. 4. It demonstrates that when the number of parameters, meaning memory consumption, is similar, it can be observed that single branch

Method	#Params (M)	Avg Acc.
LoRA	0.31	75.6
SeqLoRA	0.28	75.4
Hydra	0.28	76.5

Table 5. Comparison of LoRA, SeqLoRA, and *Hydra* on VTAB-1K benchmark. Each method is applied to both MSA and MLP blocks.

Method	#Params (M)	Avg.
LoRA	0.3	87.2
SeqLoRA	0.3	87.4
Hydra	0.3	87.9

Table 6. Comparison of LoRA, SeqLoRA, and *Hydra* on GLUE benchmark. The reported numbers represent average performance. Each method is applied to MLP blocks.

Block	#Params (M)	Avg Acc.
MSA	0.20	70.45
MLP	0.20	70.95

Table 7. Ablation results for the optimal position of *Hydra* module on the ELEVATER benchmark.

methods are generally faster than *Hydra*. However, the difference is not significant, and as observed in previous experiments, *Hydra* has demonstrated exceptional adaptation performance compared to other methods. Additionally, *Hydra* has the advantage of no additional inference latency. Therefore, the adaptation branches used for fine-tuning have no impact on the inference computational complexity.

4.5. Ablation studies

In this section, we performed ablation studies to validate the rationale behind our architecture design. First, we carried out a head-to-head comparison to fairly assess the efficacy of our approach. Next, we verified the effective position of *Hydra* in the transformer architecture. Here, we present only the summarized tables, Tabs. 5 to 7. The full tables are reported in Appendix A.

Head-to-head comparison *Hydra* is a method that combines parallel and sequential branches, i.e., LoRA and SeqLoRA. We performed experiments, ablating one of these branches, to prove the advantage of combined branch method. To do so, we leveraged the vision experiments in Sec. 4.2 and the natural language experiments in Sec. 4.3 with same experimental settings. For fair comparison, we applied each method to the blocks where the adapter module was attached in each experiment. We configured the low-rank r to ensure a similar number of trainable parameters.

As shown in Tabs. 5 and 6, *Hydra* exhibits the highest average performance in both experiments. In addition, while there is no significant difference in performance between LoRA and SeqLoRA, *Hydra* demonstrates a notable discrepancy. This observation implies that combining LoRA and SeqLoRA, *Hydra*, is more effective way than using each. Considering our analysis that parallel and sequential branch are complementary in nature, the proposed method can be regarded as effectively integrating the strengths of each branch. Consequently, the general and expressive form of our method enables outstanding fine-tuning across diverse task domains, regardless of the specific domain.

Position of Hydra module Inherently, *Hydra* module

can be applied to any linear layer of the transformer, such as projection layers of MSA blocks or linear layers that reside in MLP blocks. We mainly applied the *Hydra* module to MLP blocks, guided by the distinctive attribute of each block. To make it more concretely, we empirically investigate the optimal block for *Hydra* module. It was performed on the ELEVATER benchmark experiments in Sec. 4.1.

The results are shown in Tab. 7. We observed that when applying *Hydra* module to MLP blocks, it demonstrates better performance. Therefore, our architecture design, *Hydra*-MLP described in Fig. 2, is reasonable. Furthermore, it indicates that our method well transforms pre-trained features with amplified high-frequency by MLP block into task-specific features.

5. Conclusion

In this paper, we conduct an in-depth analysis of the roles of each adaptation branch, parallel and sequential, which has not been explored. We demonstrate that parallel branch inclines towards acquiring novel features through the exploration of absent features during pre-training phase, while the sequential branch utilizes pre-trained features to capture relatively general features.

We also propose a general and expressive adaptation formulation, *Hydra*, which combines parallel and sequential adaptation branch to integrate the capabilities of both branches. By leveraging linear adapter module, it has no additional inference latency and can be applied to any linear layer. Furthermore, thanks to its simple structure, *Hydra* can be easily implemented. The proposed method demonstrates superior performance on comprehensive experiments, including both vision and natural language tasks, without bells and whistles. This shows the versatility of *Hydra* in fine-tuning applications.

Since our focus is primarily on analyzing the characteristics of each branch and demonstrating the effectiveness of the multi-branch approach, we utilize simple linear adapter module. However, the form of *Hydra* is not influenced by the adapter module. Therefore, existing adapter-based

methods can be easily extended to multi-branch variants. We anticipate that the general and expressive formation of *Hydra* will be widely adopted in the field of the parameter efficient fine-tuning.

References

- [1] Ankur Bapna, Naveen Arivazhagan, and Orhan Firat. Simple, scalable adaptation for neural machine translation. *arXiv preprint arXiv:1909.08478*, 2019. **2**
- [2] Charles Beattie, Joel Z Leibo, Denis Teplyashin, Tom Ward, Marcus Wainwright, Heinrich Küttler, Andrew Lefrancq, Simon Green, Víctor Valdés, Amir Sadik, et al. Deepmind lab. *arXiv preprint arXiv:1612.03801*, 2016. **17**
- [3] Luisa Bentivogli, Peter Clark, Ido Dagan, and Danilo Giampiccolo. The fifth pascal recognizing textual entailment challenge. In *TAC*. Citeseer, 2009. **13**
- [4] Lukas Bossard, Matthieu Guillaumin, and Luc Van Gool. Food-101—mining discriminative components with random forests. In *Computer Vision—ECCV 2014: 13th European Conference, Zurich, Switzerland, September 6–12, 2014, Proceedings, Part VI 13*, pages 446–461. Springer, 2014. **16**
- [5] Tom Brown, Benjamin Mann, Nick Ryder, Melanie Subbiah, Jared D Kaplan, Prafulla Dhariwal, Arvind Neelakantan, Pranav Shyam, Girish Sastry, Amanda Askell, et al. Language models are few-shot learners. *Advances in neural information processing systems*, 33:1877–1901, 2020. **1, 2**
- [6] Daniel Cer, Mona Diab, Eneko Agirre, Inigo Lopez-Gazpio, and Lucia Specia. Semeval-2017 task 1: Semantic textual similarity-multilingual and cross-lingual focused evaluation. *arXiv preprint arXiv:1708.00055*, 2017. **13**
- [7] Shoufa Chen, Chongjian Ge, Zhan Tong, Jiangliu Wang, Yibing Song, Jue Wang, and Ping Luo. Adaptformer: Adapting vision transformers for scalable visual recognition. *arXiv preprint arXiv:2205.13535*, 2022. **1, 2, 5, 6**
- [8] Gong Cheng, Junwei Han, and Xiaoqiang Lu. Remote sensing image scene classification: Benchmark and state of the art. *Proceedings of the IEEE*, 105(10):1865–1883, 2017. **16, 17**
- [9] Mircea Cimpoi, Subhansu Maji, Iasonas Kokkinos, Sammy Mohamed, and Andrea Vedaldi. Describing textures in the wild. In *Proceedings of the IEEE conference on computer vision and pattern recognition*, pages 3606–3613, 2014. **16, 17**
- [10] Adam Coates, Andrew Ng, and Honglak Lee. An analysis of single-layer networks in unsupervised feature learning. In *Proceedings of the fourteenth international conference on artificial intelligence and statistics*, pages 215–223. JMLR Workshop and Conference Proceedings, 2011. **16**
- [11] Ido Dagan, Oren Glickman, and Bernardo Magnini. The pascal recognising textual entailment challenge. In *Machine Learning Challenges. Evaluating Predictive Uncertainty, Visual Object Classification, and Recognising Textual Entailment: First PASCAL Machine Learning Challenges Workshop, MLCW 2005, Southampton, UK, April 11–13, 2005, Revised Selected Papers*, pages 177–190. Springer, 2006. **13**
- [12] Mostafa Dehghani, Josip Djolonga, Basil Mustafa, Piotr Padlewski, Jonathan Heek, Justin Gilmer, Andreas Steiner, Mathilde Caron, Robert Geirhos, Ibrahim Alabdulmohsin, et al. Scaling vision transformers to 22 billion parameters. *arXiv preprint arXiv:2302.05442*, 2023. **1, 2**
- [13] Jia Deng, Wei Dong, Richard Socher, Li-Jia Li, Kai Li, and Li Fei-Fei. Imagenet: A large-scale hierarchical image database. In *2009 IEEE conference on computer vision and pattern recognition*, pages 248–255. Ieee, 2009. **2**
- [14] Li Deng. The mnist database of handwritten digit images for machine learning research [best of the web]. *IEEE signal processing magazine*, 29(6):141–142, 2012. **16**
- [15] Jacob Devlin, Ming-Wei Chang, Kenton Lee, and Kristina Toutanova. Bert: Pre-training of deep bidirectional transformers for language understanding. *arXiv preprint arXiv:1810.04805*, 2018. **1, 2**
- [16] Bill Dolan and Chris Brockett. Automatically constructing a corpus of sentential paraphrases. In *Third International Workshop on Paraphrasing (IWP2005)*, 2005. **13**
- [17] Xiaoyi Dong, Jianmin Bao, Dongdong Chen, Weiming Zhang, Nenghai Yu, Lu Yuan, Dong Chen, and Baining Guo. Cswin transformer: A general vision transformer backbone with cross-shaped windows. In *Proceedings of the IEEE/CVF Conference on Computer Vision and Pattern Recognition*, pages 12124–12134, 2022. **2**
- [18] Alexey Dosovitskiy, Lucas Beyer, Alexander Kolesnikov, Dirk Weissenborn, Xiaohua Zhai, Thomas Unterthiner, Mostafa Dehghani, Matthias Minderer, Georg Heigold, Sylvain Gelly, et al. An image is worth 16x16 words: Transformers for image recognition at scale. *arXiv preprint arXiv:2010.11929*, 2020. **2**
- [19] Mark Everingham, Luc Van Gool, Christopher KI Williams, John Winn, and Andrew Zisserman. The pascal visual object classes (voc) challenge. *International journal of computer vision*, 88:303–338, 2010. **16**
- [20] Li Fei-Fei, Rob Fergus, and Pietro Perona. Learning generative visual models from few training examples: An incremental bayesian approach tested on 101 object categories. In *2004 conference on computer vision and pattern recognition workshop*, pages 178–178. IEEE, 2004. **16, 17**
- [21] Jannik Fritsch, Tobias Kuehnl, and Andreas Geiger. A new performance measure and evaluation benchmark for road detection algorithms. In *16th International IEEE Conference on Intelligent Transportation Systems (ITSC 2013)*, pages 1693–1700. IEEE, 2013. **16, 17**
- [22] Danilo Giampiccolo, Bernardo Magnini, Ido Dagan, and William B Dolan. The third pascal recognizing textual entailment challenge. In *Proceedings of the ACL-PASCAL workshop on textual entailment and paraphrasing*, pages 1–9, 2007. **13**
- [23] Ian J Goodfellow, Yaroslav Bulatov, Julian Ibarz, Sacha Arnoud, and Vinay Shet. Multi-digit number recognition from street view imagery using deep convolutional neural networks. *arXiv preprint arXiv:1312.6082*, 2013. **16, 17**
- [24] Ian J Goodfellow, Dumitru Erhan, Pierre Luc Carrier, Aaron Courville, Mehdi Mirza, Ben Hamner, Will Cukierski, Yichuan Tang, David Thaler, Dong-Hyun Lee, et al. Challenges in representation learning: A report on three machine learning contests. In *Neural Information Processing:*

- 20th International Conference, ICONIP 2013, Daegu, Korea, November 3-7, 2013. *Proceedings, Part III 20*, pages 117–124. Springer, 2013. **16**
- [25] Ben Graham. Kaggle diabetic retinopathy detection competition report. *University of Warwick*, 22, 2015. **17**
- [26] Demi Guo, Alexander M Rush, and Yoon Kim. Parameter-efficient transfer learning with diff pruning. *arXiv preprint arXiv:2012.07463*, 2020. **3**
- [27] R Bar Haim, Ido Dagan, Bill Dolan, Lisa Ferro, Danilo Giampiccolo, Bernardo Magnini, and Idan Szpektor. The second pascal recognising textual entailment challenge. In *Proceedings of the Second PASCAL Challenges Workshop on Recognising Textual Entailment*, volume 7, 2006. **13**
- [28] Kaiming He, Xinlei Chen, Saining Xie, Yanghao Li, Piotr Dollár, and Ross Girshick. Masked autoencoders are scalable vision learners. In *Proceedings of the IEEE/CVF Conference on Computer Vision and Pattern Recognition*, pages 16000–16009, 2022. **2**
- [29] Xuehai He, Chunyuan Li, Pengchuan Zhang, Jianwei Yang, and Xin Eric Wang. Parameter-efficient fine-tuning for vision transformers. *arXiv preprint arXiv:2203.16329*, 2022. **2, 3, 5, 13**
- [30] Patrick Helber, Benjamin Bischke, Andreas Dengel, and Damian Borth. Eurosat: A novel dataset and deep learning benchmark for land use and land cover classification. *IEEE Journal of Selected Topics in Applied Earth Observations and Remote Sensing*, 12(7):2217–2226, 2019. **16, 17**
- [31] Jonathan Ho, Ajay Jain, and Pieter Abbeel. Denoising diffusion probabilistic models. *Advances in Neural Information Processing Systems*, 33:6840–6851, 2020. **2**
- [32] Neil Houlsby, Andrei Giurgiu, Stanislaw Jastrzebski, Bruna Morrone, Quentin De Laroussilhe, Andrea Gesmundo, Mona Attariyan, and Sylvain Gelly. Parameter-efficient transfer learning for nlp. In *International Conference on Machine Learning*, pages 2790–2799. PMLR, 2019. **1, 2, 5, 6**
- [33] Edward J Hu, Yelong Shen, Phillip Wallis, Zeyuan Allen-Zhu, Yuanzhi Li, Shean Wang, Lu Wang, and Weizhu Chen. Lora: Low-rank adaptation of large language models. *arXiv preprint arXiv:2106.09685*, 2021. **1, 2, 3, 5, 6, 7, 13**
- [34] Menglin Jia, Luming Tang, Bor-Chun Chen, Claire Cardie, Serge Belongie, Bharath Hariharan, and Ser-Nam Lim. Visual prompt tuning. In *Computer Vision—ECCV 2022: 17th European Conference, Tel Aviv, Israel, October 23–27, 2022, Proceedings, Part XXXIII*, pages 709–727. Springer, 2022. **1, 3, 6**
- [35] Shibo Jie and Zhi-Hong Deng. Fact: Factor-tuning for lightweight adaptation on vision transformer. In *Proceedings of the AAAI Conference on Artificial Intelligence*, volume 37, pages 1060–1068, 2023. **3, 5, 6**
- [36] Justin Johnson, Bharath Hariharan, Laurens Van Der Maaten, Li Fei-Fei, C Lawrence Zitnick, and Ross Girshick. Clevr: A diagnostic dataset for compositional language and elementary visual reasoning. In *Proceedings of the IEEE conference on computer vision and pattern recognition*, pages 2901–2910, 2017. **17**
- [37] Rabeeh Karimi Mahabadi, James Henderson, and Sebastian Ruder. Compacter: Efficient low-rank hypercomplex adapter layers. *Advances in Neural Information Processing Systems*, 34:1022–1035, 2021. **2, 5**
- [38] Tero Karras, Samuli Laine, and Timo Aila. A style-based generator architecture for generative adversarial networks. In *Proceedings of the IEEE/CVF conference on computer vision and pattern recognition*, pages 4401–4410, 2019. **2**
- [39] Douwe Kiela, Hamed Firooz, Aravind Mohan, Vedanuj Goswami, Amanpreet Singh, Pratik Ringshia, and Davide Testuggine. The hateful memes challenge: Detecting hate speech in multimodal memes. *Advances in Neural Information Processing Systems*, 33:2611–2624, 2020. **16**
- [40] Alexander Kirillov, Eric Mintun, Nikhila Ravi, Hanzi Mao, Chloe Rolland, Laura Gustafson, Tete Xiao, Spencer Whitehead, Alexander C Berg, Wan-Yen Lo, et al. Segment anything. *arXiv preprint arXiv:2304.02643*, 2023. **1**
- [41] Jonathan Krause, Michael Stark, Jia Deng, and Li Fei-Fei. 3d object representations for fine-grained categorization. In *Proceedings of the IEEE international conference on computer vision workshops*, pages 554–561, 2013. **16**
- [42] Alex Krizhevsky et al. Learning multiple layers of features from tiny images. 2009. **2, 16, 17**
- [43] Yann LeCun, Fu Jie Huang, and Leon Bottou. Learning methods for generic object recognition with invariance to pose and lighting. In *Proceedings of the 2004 IEEE Computer Society Conference on Computer Vision and Pattern Recognition, 2004. CVPR 2004.*, volume 2, pages II–104. IEEE, 2004. **17**
- [44] Brian Lester, Rami Al-Rfou, and Noah Constant. The power of scale for parameter-efficient prompt tuning. *arXiv preprint arXiv:2104.08691*, 2021. **3**
- [45] Mike Lewis, Yinhan Liu, Naman Goyal, Marjan Ghazvininejad, Abdelrahman Mohamed, Omer Levy, Ves Stoyanov, and Luke Zettlemoyer. Bart: Denoising sequence-to-sequence pre-training for natural language generation, translation, and comprehension. *arXiv preprint arXiv:1910.13461*, 2019. **2**
- [46] Chunyuan Li, Haotian Liu, Liunian Li, Pengchuan Zhang, Jyoti Aneja, Jianwei Yang, Ping Jin, Houdong Hu, Zicheng Liu, Yong Jae Lee, et al. Elevator: A benchmark and toolkit for evaluating language-augmented visual models. *Advances in Neural Information Processing Systems*, 35:9287–9301, 2022. **5, 13**
- [47] Xiang Lisa Li and Percy Liang. Prefix-tuning: Optimizing continuous prompts for generation. *arXiv preprint arXiv:2101.00190*, 2021. **1, 3**
- [48] Dongze Lian, Daquan Zhou, Jiashi Feng, and Xinchao Wang. Scaling & shifting your features: A new baseline for efficient model tuning. *Advances in Neural Information Processing Systems*, 35:109–123, 2022. **1, 3, 5, 6**
- [49] Tsung-Yi Lin, Michael Maire, Serge Belongie, James Hays, Pietro Perona, Deva Ramanan, Piotr Dollár, and C Lawrence Zitnick. Microsoft coco: Common objects in context. In *Computer Vision—ECCV 2014: 13th European Conference, Zurich, Switzerland, September 6–12, 2014, Proceedings, Part V 13*, pages 740–755. Springer, 2014. **2**
- [50] Yinhan Liu, Myle Ott, Naman Goyal, Jingfei Du, Mandar Joshi, Danqi Chen, Omer Levy, Mike Lewis, Luke Zettlemoyer, and Veselin Stoyanov. Roberta: A robustly optimized

- bert pretraining approach. *arXiv preprint arXiv:1907.11692*, 2019. [2](#), [6](#)
- [51] Ze Liu, Yutong Lin, Yue Cao, Han Hu, Yixuan Wei, Zheng Zhang, Stephen Lin, and Baining Guo. Swin transformer: Hierarchical vision transformer using shifted windows. In *Proceedings of the IEEE/CVF international conference on computer vision*, pages 10012–10022, 2021. [2](#)
- [52] Gen Luo, Minglang Huang, Yiyi Zhou, Xiaoshuai Sun, Guannan Jiang, Zhiyu Wang, and Rongrong Ji. Towards efficient visual adaption via structural re-parameterization. *arXiv preprint arXiv:2302.08106*, 2023. [3](#), [4](#), [5](#), [6](#)
- [53] Subhransu Maji, Esa Rahtu, Juho Kannala, Matthew Blaschko, and Andrea Vedaldi. Fine-grained visual classification of aircraft. *arXiv preprint arXiv:1306.5151*, 2013. [16](#)
- [54] Loic Matthey, Irina Higgins, Demis Hassabis, and Alexander Lerchner. dsprites: Disentanglement testing sprites dataset, 2017. [17](#)
- [55] Maria-Elena Nilsback and Andrew Zisserman. Automated flower classification over a large number of classes. In *2008 Sixth Indian Conference on Computer Vision, Graphics & Image Processing*, pages 722–729. IEEE, 2008. [16](#), [17](#)
- [56] Namuk Park and Songkuk Kim. How do vision transformers work? *arXiv preprint arXiv:2202.06709*, 2022. [4](#)
- [57] Omkar M Parkhi, Andrea Vedaldi, Andrew Zisserman, and CV Jawahar. Cats and dogs. In *2012 IEEE conference on computer vision and pattern recognition*, pages 3498–3505. IEEE, 2012. [16](#), [17](#)
- [58] Jonas Pfeiffer, Aishwarya Kamath, Andreas Rücklé, Kyunghyun Cho, and Iryna Gurevych. Adapterfusion: Non-destructive task composition for transfer learning. *arXiv preprint arXiv:2005.00247*, 2020. [2](#)
- [59] Alec Radford, Jong Wook Kim, Chris Hallacy, Aditya Ramesh, Gabriel Goh, Sandhini Agarwal, Girish Sastry, Amanda Askell, Pamela Mishkin, Jack Clark, et al. Learning transferable visual models from natural language supervision. In *International conference on machine learning*, pages 8748–8763. PMLR, 2021. [2](#), [16](#)
- [60] Alec Radford, Jeffrey Wu, Rewon Child, David Luan, Dario Amodei, Ilya Sutskever, et al. Language models are unsupervised multitask learners. *OpenAI blog*, 1(8):9, 2019. [2](#)
- [61] Colin Raffel, Noam Shazeer, Adam Roberts, Katherine Lee, Sharan Narang, Michael Matena, Yanqi Zhou, Wei Li, and Peter J Liu. Exploring the limits of transfer learning with a unified text-to-text transformer. *The Journal of Machine Learning Research*, 21(1):5485–5551, 2020. [1](#), [2](#)
- [62] Pranav Rajpurkar, Jian Zhang, Konstantin Lopyrev, and Percy Liang. Squad: 100,000+ questions for machine comprehension of text. *arXiv preprint arXiv:1606.05250*, 2016. [13](#)
- [63] Sylvestre-Alvise Rebuffi, Hakan Bilen, and Andrea Vedaldi. Learning multiple visual domains with residual adapters. *Advances in neural information processing systems*, 30, 2017. [2](#)
- [64] Andreas Rücklé, Gregor Geigle, Max Glockner, Tilman Beck, Jonas Pfeiffer, Nils Reimers, and Iryna Gurevych. Adapterdrop: On the efficiency of adapters in transformers. *arXiv preprint arXiv:2010.11918*, 2020. [2](#), [6](#)
- [65] Mark Sandler, Andrey Zhmoginov, Max Vladymyrov, and Andrew Jackson. Fine-tuning image transformers using learnable memory. In *Proceedings of the IEEE/CVF Conference on Computer Vision and Pattern Recognition*, pages 12155–12164, 2022. [3](#)
- [66] Richard Socher, Alex Perelygin, Jean Wu, Jason Chuang, Christopher D Manning, Andrew Y Ng, and Christopher Potts. Recursive deep models for semantic compositionality over a sentiment treebank. In *Proceedings of the 2013 conference on empirical methods in natural language processing*, pages 1631–1642, 2013. [13](#)
- [67] Johannes Stalkamp, Marc Schlipfing, Jan Salmen, and Christian Igel. The german traffic sign recognition benchmark: a multi-class classification competition. In *The 2011 international joint conference on neural networks*, pages 1453–1460. IEEE, 2011. [16](#)
- [68] Yi-Lin Sung, Jaemin Cho, and Mohit Bansal. VI-adapter: Parameter-efficient transfer learning for vision-and-language tasks. In *Proceedings of the IEEE/CVF Conference on Computer Vision and Pattern Recognition*, pages 5227–5237, 2022. [2](#)
- [69] Hugo Touvron, Matthieu Cord, Matthijs Douze, Francisco Massa, Alexandre Sablayrolles, and Hervé Jégou. Training data-efficient image transformers & distillation through attention. In *International conference on machine learning*, pages 10347–10357. PMLR, 2021. [2](#)
- [70] Laurens Van der Maaten and Geoffrey Hinton. Visualizing data using t-sne. *Journal of machine learning research*, 9(11), 2008. [7](#)
- [71] Ashish Vaswani, Noam Shazeer, Niki Parmar, Jakob Uszkoreit, Llion Jones, Aidan N Gomez, Łukasz Kaiser, and Illia Polosukhin. Attention is all you need. *Advances in neural information processing systems*, 30, 2017. [2](#)
- [72] Bastiaan S Veeling, Jasper Linmans, Jim Winkens, Taco Cohen, and Max Welling. Rotation equivariant cnns for digital pathology. In *Medical Image Computing and Computer Assisted Intervention—MICCAI 2018: 21st International Conference, Granada, Spain, September 16–20, 2018, Proceedings, Part II 11*, pages 210–218. Springer, 2018. [16](#), [17](#)
- [73] Alex Wang, Yada Pruksachatkun, Nikita Nangia, Amanpreet Singh, Julian Michael, Felix Hill, Omer Levy, and Samuel Bowman. Superglue: A stickier benchmark for general-purpose language understanding systems. *Advances in neural information processing systems*, 32, 2019. [6](#)
- [74] Alex Wang, Amanpreet Singh, Julian Michael, Felix Hill, Omer Levy, and Samuel R Bowman. Glue: A multi-task benchmark and analysis platform for natural language understanding. *arXiv preprint arXiv:1804.07461*, 2018. [13](#)
- [75] Peihao Wang, Wenqing Zheng, Tianlong Chen, and Zhangyang Wang. Anti-oversmoothing in deep vision transformers via the fourier domain analysis: From theory to practice. *arXiv preprint arXiv:2203.05962*, 2022. [4](#)
- [76] Alex Warstadt, Amanpreet Singh, and Samuel R Bowman. Neural network acceptability judgments. *arXiv preprint arXiv:1805.12471*, 2018. [13](#)
- [77] Adina Williams, Nikita Nangia, and Samuel R Bowman. A broad-coverage challenge corpus for sentence understanding

- through inference. *arXiv preprint arXiv:1704.05426*, 2017. [13](#)
- [78] Thomas Wolf, Lysandre Debut, Victor Sanh, Julien Chaumond, Clement Delangue, Anthony Moi, Pierric Cistac, Tim Rault, Rémi Louf, Morgan Funtowicz, et al. Transformers: State-of-the-art natural language processing. In *Proceedings of the 2020 conference on empirical methods in natural language processing: system demonstrations*, pages 38–45, 2020. [6](#)
- [79] Jianxiong Xiao, James Hays, Krista A Ehinger, Aude Oliva, and Antonio Torralba. Sun database: Large-scale scene recognition from abbey to zoo. In *2010 IEEE computer society conference on computer vision and pattern recognition*, pages 3485–3492. IEEE, 2010. [16](#), [17](#)
- [80] Elad Ben Zaken, Shauli Ravfogel, and Yoav Goldberg. Bitfit: Simple parameter-efficient fine-tuning for transformer-based masked language-models. *arXiv preprint arXiv:2106.10199*, 2021. [1](#), [3](#), [6](#)
- [81] Xiaohua Zhai, Joan Puigcerver, Alexander Kolesnikov, Pierre Ruysen, Carlos Riquelme, Mario Lucic, Josip Djolonga, Andre Susano Pinto, Maxim Neumann, Alexey Dosovitskiy, et al. The visual task adaptation benchmark. 2019. [5](#), [13](#)
- [82] Qingru Zhang, Minshuo Chen, Alexander Bukharin, Pengcheng He, Yu Cheng, Weizhu Chen, and Tuo Zhao. Adaptive budget allocation for parameter-efficient fine-tuning. *arXiv preprint arXiv:2303.10512*, 2023. [2](#), [3](#)
- [83] Yuanhan Zhang, Kaiyang Zhou, and Ziwei Liu. Neural prompt search. *arXiv preprint arXiv:2206.04673*, 2022. [6](#)
- [84] Bolei Zhou, Hang Zhao, Xavier Puig, Sanja Fidler, Adela Barriuso, and Antonio Torralba. Scene parsing through ade20k dataset. In *Proceedings of the IEEE conference on computer vision and pattern recognition*, pages 633–641, 2017. [2](#)

Hydra: Multi-head Low-rank Adaptation for Parameter Efficient Fine-tuning

Appendix

A. Detailed results of ablation studies

Due to constraints of space, we reported only the summarized tables in the main paper. Here, we present full results for each experiment.

- Tab. 8: The detailed results of head-to-head comparison on VTAB-1k benchmark.
- Tab. 9: The detailed results of head-to-head comparison on GLUE benchmark.
- Tab. 10: The detailed results of the optimal position of *Hydra* module experiment on ELEVATER benchmark.

B. Experimental details

B.1. Few-shot experiments

Following [29], we used SGD optimizer to fine-tune the model. We set $r_a = r_b = 2$ for the *Hydra* module since the rank of the LoRA in this experiment is set to 4. We searched for the optimal learning rate and the weight decay using the automatic hyper-parameter tuning toolkit from ELEVATER [46]. Every experiments of few-shot setting on the ELEVATER benchmark are conducted on a single NVIDIA-A100 GPU. We report the hyper-parameters in Tab. 11.

B.2. VTAB-1k experiments

We used AdamW optimizer with cosine scheduler where warm-up epoch is set to 10. For the similar number of parameters compared with methods in benchmark, we set low ranks $r_a = r_b = 2$ in both MSA and MLP blocks. *Hydra* is trained with 100 epochs for all datasets. Detailed hyper-parameters for each dataset are reported in Tab. 12. All of the results are conducted on a single NVIDIA-A100 GPU.

B.3. Natural language understanding experiments

We used AdamW optimizer with a linear learning rate decay schedule and set warm-up iteration ratio as 0.06. Across the datasets, the low ranks are set as $r_a = 4$ and $r_b = 8$. Following LoRA [33], the adaptation modules for the MRPC, RTE and STS-B experiments were initialized using the best MNLI experiment checkpoint. The hyper-parameters specific to each dataset are presented in Table 13. We used 4 NVIDIA-A100 GPUs for training.

C. Dataset details

C.1. Few-shot experiments

We tested Hydra on 20 datasets from ELEVATER benchmark [46] for few-shot experiments: Caltech101, CIFAR10, CIFAR100, Country211, DTD, EuroSat, FER2013, FGVC Aircraft, Food101, GTSRB, HatefulMememes, KittiDistance, MNIST, Flowers102, OxfordPets, PatchCamelyon, SST2, RESISC45, StanfordCars, and VOC2007. Detailed statistics of each dataset are reported in Tab. 14.

C.2. VTAB-1k experiments

We assessed the accuracy using the VTAB-1k benchmark [81], and the statistics of each dataset are presented in Tab. 15. The benchmark consists of various vision domain with three groups: CIFAR100, Caltech101, DTD, Flowers102, OxfordPets, SVHN and SUN397 in *Natural* group, PatchCamelyon, EuroSAT, Resisc45 and Retinopathy in *Specialized* group, and Clevr, DMLab, dSprites and SmallNORB in *Structured* group. The number of train data is fixed to 1,000 for each dataset.

C.3. Natural language understanding experiments

We evaluated our method on the General Language Understanding Evaluation (GLUE) benchmark [74]. It covers various language understanding tasks, including linguistic acceptability (CoLA [76]), sentiment analysis (SST-2 [66]), paraphrase (MRPC [16], QQP²), sentence similarity (STS-B [6]), and natural language inference (MNLI [77], QNLI [62], RTE [3, 11, 22, 27]).

²data.quora.com/First-Quora-Dataset-Release-Question-Pairs

Method	#Params(M)	Avg. Acc.	Natural							Specialized				Structured							
			CIFAR100	Caltech101	DTD	Flowers102	OxfordPets	SVHN	Sun397	PatchCamelyon	EuroSAT	Resisc45	Retinopathy	Clevr-Count	Clevr-Dist	DMLab	KITTI-Dist	dSPR-Loc	dSPR-Ori	sNORB-Azim	sNORB-Ele
LoRA	0.31	75.6	72.86	90.5	73.2	99.3	91.4	88.4	55.0	85.6	94.4	85.9	74.4	81.5	68.2	49.4	78.6	78.5	49.5	32.7	43.0
SeqLoRA	0.28	75.4	72.4	89.2	71.4	99.0	90.8	87.7	55.2	85.6	94.3	84.9	74.7	82.7	67.7	49.3	79.9	81.0	50.1	32.8	40.3
Hydra	0.28	76.5	72.7	91.3	72.0	99.2	91.4	90.7	55.5	85.8	96.0	86.1	75.9	83.2	68.2	50.9	82.3	80.3	50.8	34.5	43.1

Table 8. The detailed results of head-to-head comparison on VTAB-1k benchmark.

Method	#Params(M)	Avg.	MNLI	SST-2	MRPC	CoLA	QNLI	QQP	RTE	STS-B
LoRA	0.3	87.2	87.2	94.5	90.2	64.2	92.5	90.7	87.4	91.1
SeqLoRA	0.3	87.4	87.5	94.7	90.7	63.3	93.0	90.8	88.1	91.4
Hydra	0.3	87.9	87.5	95.0	92.2	65.4	92.8	90.8	87.4	91.7

Table 9. The detailed results of head-to-head comparison on GLUE benchmark.

Method	#Params(M)	Avg. Acc.(↑)	Caltech101	CIFAR10	CIFAR100	Country211	DTD	EuroSAT	FER2013	FGVCAircraft	Food101	GTSRB	HatefulMemes	KITTI-Dist	MNIST	Flowers102	OxfordPets	PatchCamelyon	SST2	Resisc45	StanfordCars	VOC2007
MSA	0.20	70.45	92.01	90.76	73.93	17.65	65.05	81.60	51.32	32.00	84.37	85.66	55.90	43.74	91.47	92.56	89.37	68.85	59.80	79.80	69.95	83.16
MLP	0.20	70.95	91.23	90.89	74.20	17.75	64.47	87.00	51.10	33.05	84.27	87.11	55.91	42.05	90.76	93.18	89.38	70.83	59.58	82.41	71.19	82.66

Table 10. The detailed results of the optimal position of *Hydra* module experiment on ELEVATER benchmark.

Method	Caltech101	CIFAR10	CIFAR100	Country211	DTD	EuroSAT	FER2013	FGVCAircraft	Food101	GTSRB	HatefulMemes	KITTI-Dist	MNIST	Flowers102	OxfordPets	PatchCamelyon	SST2	Resisc45	StanfordCars	VOC2007		
Batch size	64	64	64	64	64	64	64	64	64	64	64	64	64	64	64	64	64	64	64	64	64	
Epochs	50	50	50	50	50	50	50	50	50	50	50	50	50	50	50	50	50	50	50	50	50	50
Learning rate	1e-2	1e-3	1e-3	1e-3	1e-2	1e-2	1e-2	1e-2	1e-4	1e-1	1e-4	1e-2	1e-2	1e-2	1e-2	1e-2	1e-4	1e-2	1e-2	1e-2	1e-1	1e-1
Weight decay	3.16e-4	1.00e-6	1.00e+0	1.33e-6	1.00e-6	1.00e-6	1.00e-4	3.16e-6	1.00e-4	1.00e-2	1.00e+4	1.00e-6	1.00e-6	1.00e-6	1.00e-6	1.00e+0	1.00e-6	1.00e-4	3.16e-4	3.16e-1	3.16e-1	3.16e-1

Table 11. The hyper-parameters in few-shot experiments. Since the weight decays for each dataset are searched in the logspace, we report them using two significant digits in the exponential notation.

Hyper-parameter	CIFAR100	Caltech101	DTD	Flower102	Pets	SVHN	Sun397	Camelyon	EuroSAT	Resisc45	Retinopathy	Clevr-Count	Clevr-Dist	DMLab	KITTI-Dist	dSPR-Loc	dSPR-Ori	sNORB-Azim	sNORB-Ele
Batch size	16	32	32	64	32	16	64	64	16	64	64	64	16	64	64	16	64	64	64
Learning rate	5e-4	1e-3	1e-3	5e-3	1e-3	1e-3	1e-3	5e-3	5e-4	5e-3	5e-4	5e-4	5e-4	1e-3	5e-4	1e-3	1e-3	5e-3	5e-4
Weight decay	1e-4	1e-4	1e-4	1e-4	1e-4	1e-4	1e-4	1e-4	1e-4	1e-4	1e-4	1e-4	1e-4	1e-4	1e-4	1e-4	1e-4	1e-5	1e-4
Dropout	0.2	0.1	0.2	0.0	0.0	0.0	0.2	0.2	0.0	0.2	0.2	0.2	0.0	0.2	0.2	0.2	0.2	0.2	0.2

Table 12. The hyper-parameters in VTAB-1k experiments.

Hyper-parameter	MNLI	SST-2	MRPC	CoLA	QNLI	QQP	RTE	STS-B
Batch size	8	16	16	4	8	16	16	4
Epochs	30	60	40	80	25	25	80	40
Learning rate	4e-4	6e-4	6e-4	4e-4	8e-4	6e-4	8e-4	6e-4
Weight decay	0.1	0.1	0.1	0.1	0.1	0.1	0.2	0.1

Table 13. The hyper-parameters in NLU experiments.

Dataset	#labels	Train size	Test size
Hateful Memes [39]	2	8,500	500
PatchCamelyon [72]	2	262,144	32,768
Rendered-SST2 [59]	2	6,920	1,821
KITTI Distance [21]	4	6,347	711
FER 2013 [24]	7	28,709	3,589
CIFAR10 [42]	10	50,000	10,000
EuroSAT [30]	10	5,000	5,000
MNIST [14]	10	60,000	10,000
STL10 [10]	10	5,000	8,000
SVHN [23]	10	73,257	26,032
VOC 2007 Classification [19]	20	2,501	4,952
Oxford-IIIT-Pets [57]	37	3,680	3,669
GTSRB [67]	43	26,640	12,630
Resisc45 [8]	45	3,150	25,200
Describable Textures [9]	47	1,880	1,880
CIFAR100 [42]	100	50,000	10,000
FGVC Aircraft [53]	100	3,334	3,333
Food101 [4]	101	75,750	25,250
Caltech101 [20]	101	3,060	6,084
Oxford-Flowers102 [55]	102	1,020	6,149
Stanford Cars [41]	196	8,144	8,041
Country-211 [59]	211	31,650	21,100
SUN397 [79]	397	19,850	19,850

Table 14. Statistics of 23 datasets used in few-shot experiments.

Dataset	#labels	Train size	Test size
CIFAR100 [42]	100		10,000
Caltech101 [20]	102		6,084
Describable Textures [9]	47		1,880
Oxford-Flowers102 [55]	102		6,149
Oxford-IIIT-Pets [57]	37		3,669
SVHN [23]	10		26,032
Sun397 [79]	397		36,032
PatchCamelyon [72]	2		32,768
EuroSAT [30]	10		5,400
Resisc45 [8]	45	1,000	6,300
Retinopathy [25]	5		42,670
Clevr/count [36]	8		15,000
Clevr/distance [36]	6		15,000
DMLab [2]	6		22,735
KITTI Distance [21]	4		711
dSprites/location [54]	16		73,728
dSprites/orientation [54]	16		73,728
SmallNORB/azimuth [43]	18		12,150
SmallNORB/elevation [43]	18		12,150

Table 15. Datasets of VTAB-1k benchmark